# Preparation of Organic−Inorganic Nanocomposites with a Layered Titanate

Nipaka Sukpirom and Michael M. Lerner*

*Department of Chemistry and Center for Advanced Materials Research, Oregon State University, Corvallis, Oregon 97331-4003*

*Received February 6, 2001. Revised Manuscript Received April 6, 2001*

Layered nanocomposites with poly(ethylene oxide), PEO, and poly(vinylpyrrolidone), PVP, incorporated between $H_xTi_{2-x/4}\square_{x/4}O_4$ ($\square$ = Ti vacancy) titanate layers, are synthesized from a colloidal titanate suspension obtained by exfoliation in aqueous tetrabutylammonium hydroxide and subsequent acidification. Products are characterized by powder X-ray diffraction, thermal analyses, FTIR spectroscopy, scanning electron microscopy, and elemental analysis. Interlayer expansions for the vacuum-dried nanocomposites are 0.81 and 2.2 nm for the PEO- and PVP-containing products, respectively. Both nanocomposites are comprised of 10−100-$\mu$m diameter platelets, much larger than those of 0.1−1 $\mu$m for the starting titanate. FTIR spectra indicate the presence of the polymers and suggest decreased water interaction with titanate sheet surfaces for the polymer-containing products. Thermal analyses of nanocomposites show intercalate water loss below 200 °C, polymer degradation and structure decomposition between 200 and 450 °C, and a titanate phase change above 450 °C. Elemental analyses give empirical formulas of $H_{0.7}Ti_{1.83}O_4(C_2H_4O)_{1.54}(H_2O)_{1.28}$ and $H_{0.7}Ti_{1.83}O_4(C_{16}H_{36}N)_{0.05}(C_6H_9NO)_{1.22}(H_2O)_{0.92}$ for the PEO and PVP nanocomposites, respectively. These results are compared with those obtained for other layered nanocomposites.

## Introduction

A wide range of polymers and hosts have been combined to form nanocomposite structures, and nanostructured materials have been shown to exhibit novel, and technologically useful, mechanical, optical, electrical, and barrier properties.[1−3] Layered nanocomposites are materials generally comprised of an organic polymer incorporated between sheets of an inorganic host. Much research has been devoted to developing new synthetic methods for these materials: layered nanocomposites have been prepared by the in situ polymerization of intercalated monomers, the exfoliation of a layered host and subsequent adsorption of polymer and reaggregation, template syntheses of host structures in polymer-containing solutions, and direct melt intercalation of polymers into hosts.[4−6]

Table 1 provides a selected summary indicating the range of different hosts that have been studied in layered nanocomposites. By far, the most work has concentrated on the aluminosilicate smectite clays such as montmorillonite and hectorite. These hosts have a number of advantages in this application. First, they spontaneously delaminate in appropriate aqueous conditions and are also amenable to melt intercalation,[5] greatly facilitating the preparation of nanocomposites. Aluminosilicate clays are also inexpensive, nontoxic, and refractory and can be surface-modified. Clay-based nanocomposites have therefore shown properties that indicate commercial potential as structural materials,[2,29−31] UV barrier coatings,[31] gas barrier coatings,[31,32] and fire retardants.[33]

Nanostructures based on $TiO_2$ are a very attractive prospect due to the low cost, environmental accept-

**Table 1. Selected List of Inorganic Hosts Studied in Layered Nanocomposites with Poly(ethyleneoxide), PEO, and Poly(vinylpyrrolidone), PVP**

| host | polymer | reference |
|---|---|---|
| smectite clays | PEO | 5, 7−9 |
| | PVP | 10−13 |
| $MoO_3$ | PEO | 14−17 |
| | PVP | 16 |
| $V_2O_5$ | PEO | 18 |
| $MoS_2$ | PEO | 19−21 |
| $NbSe_2$ | PEO | 22 |
| | PVP | 22 |
| $MPS_3$ | PEO | 14, 23−25 |
| | PVP | 23 |
| $RuCl_3$ | PEO | 26 |
| | PVP | 26 |
| graphite oxide | PEO | 27, 28 |

(1) Lerf, A. Intercalation Compounds in Layered Host Lattices: Supramolecular Chemistry in Nanodimensions. In *Handbook of Nanostructured Materials and Nanotechnology*; Nalwa, H., Ed.; Academic Press: New York, 2000; Vol. 5, pp 1−166.
(2) LeBaron, P.; Wang, Z.; Pinnavaia, T. *Appl. Clay Sci.* **1999**, *15*, 11.
(3) Sanchez, C.; Ribot, F.; Lebeau, B. *J. Mater. Chem.* **1999**, *9*, 35.
(4) Lerner, M.; Oriakhi, C. Polymers in Ordered Nanocomposites. In *Handbook of Nanophase Materials*; Goldstein, A., Ed.; Marcel Dekker: New York, 1997; pp 199−219.
(5) Gianellis, E. P. *Adv. Mater.* **1996**, *8*, 29.
(6) Oriakhi, C. *J. Chem. Ed.* **2000**, *77*, 1138.
(7) Bujdak, J.; Hackett, E.; Giannelis, E. P. *Chem. Mater.* **2000**, *12*, 2168.
(8) Aranda, P.; Ruiz-Hitzky, E. *Appl. Clay. Sci.* **1999**, *15*, 119.

10.1021/cm0101226 CCC: $20.00 
Published on Web 05/30/2001

ability, chemical stability, and photochemical properties of $TiO_2$ and many titanates. As with other inorganic solids, the optical properties of $TiO_2$ have been modified by preparing nanoparticles.[34−36] Composite materials comprising nanostructured $TiO_2$ have also been examined; a polyimide matrix with nanostructured titania has been reported and proposed for use in waveguides.[37] A $TiO_2$ nanocomposite with PVP was prepared by a sol−gel method via hydrolysis of a titanium alkoxide.[38] This method produced a disordered titania network homogeneously dispersed in PVP.

Hervieu and Raveau originally reported a series of nonstoichiometric layered titanates, $A_xTi_{2-x/4}\square_{x/4}O_4{\cdot}H_2O$ (A = Li−Cs or H, $x = 0.67-0.73$, □ indicates vacant Ti sites) with a lepidocrocite-like structure.[39] In the past few years, Sasaki and co-workers prepared and characterized protonated and exfoliated forms of these materials.[36,40−44] A mixed-metal sheet structure with Li substitution in the Ti sites, $A_xTi_{2-x/3}Li_{x/3}O_4$ (A = K−Cs or H, $x = 0.7-0.8$), has also been reported by the same group.[45] The proton-exchanged form of the first structure, $H_{0.7}Ti_{1.83}\square_{0.17}O_4{\cdot}0.7H_2O$ (H−Ti), swells and then delaminates in aqueous solutions containing tetrabutylammonium (TBA) cations.[41−44] Detailed XRD and optical characterization of the resulting colloidal suspensions have clearly demonstrated that when the mole ratio of TBA to protons in H−Ti (TBA/H) exceeds 0.5, the titania sheet galleries swell with water to the extent that a majority or all of the titanate layers become exfoliated into individually suspended sheets in the solution.[42−44] The complete exfoliation process occurs simply by stirring in the TBA-containing aqueous solution and requires several days; the reaction is most favorable when high (5/1) TBA/H ratios are used.[41,44]

Recent work by Sasaki et al. demonstrated that multilayer thin films of titania nanosheets can be prepared via a layer-by-layer self-assembly approach.[46] Repeated immersions of a substrate in solutions of the colloidal titania suspension followed by poly(dimethyldiallylammonium chloride) (PDDACl) resulted in the deposition of thin films containing 0.65-nm PDDA layers between individual titania layers.

We here report the application of the colloidal suspensions of exfoliated titania sheets as precursors to form lamellar titania nanocomposites with PEO and PVP and the structural and compositional characterization of these new materials by XRD, TGA, DSC, FTIR, and elemental analyses.

## Experimental Section

**Materials.** Tetrabutylammonium hydroxide (Aldrich, 40% in water), $TiO_2$ (Aldrich, anatase form, 99.9+%), $Cs_2CO_3$ (Aldrich, 99.9%), poly(ethylene oxide) (PEO, Aldrich, $M_n$ = 100 000) and poly(vinylpyrrolidone) (PVP, Aldrich, $M_n$ = 40 000) were used as received. $Cs_xTi_{2-x/4}\square_{x/4}O_4{\cdot}yH_2O$, abbreviated Cs−Ti, was prepared according to a literature method.[39] Anatase $TiO_2$ (4.23 g) and $Cs_2CO_3$ (3.26 g) were ground together and heated briefly at 800 °C in an alumina crucible to eliminate $CO_2$. The mixture was reground and reheated at 800 °C twice for 20 h. The proton-exchanged material, $H_xTi_{2-x/4}\square_{x/4}O_4{\cdot}yH_2O$ ($x \approx 0.7$, $y \approx 1$), abbreviated H−Ti, was prepared by stirring Cs−Ti powder in 100 mL of 1 M HCl for 48 h, with the solution replaced after 24 h. Powder X-ray diffraction (XRD) indicated that the proton exchange reaction was complete and both solid products matched those described previously.[40,47]

**H−Ti Exfoliation.** H−Ti (0.25 g) was added to an aqueous solution of tetrabutylammonium (TBA) hydroxide (50 mL) in a 100-mL glass bottle, maintaining a 0.5 mol/mol ratio of TBA to protons in H−Ti. The sample was prepared using a GE600 ultrasonic processor with a titanium alloy probe (13-mm diameter) for 20 min at settings of 600 W/30% amplitude. After ultrasonication, the exfoliated H−Ti layers were suspended in the solution, and no solid could be isolated by filtration on 11-$\mu$m pore diameter paper (Whatman #1). The reaggregated colloid was obtained by freeze-drying the solution for 24 h (Virtis Research Equipment freeze-dryer) and has composition $H_xTBA_{1-x}Ti_{2-x/4}\square_{x/4}O_4{\cdot}yH_2O$ ($x \approx 0.7$, $y \approx 1$), abbreviated as TBA/H−Ti.

**Preparation of PEO/H−Ti and PVP/H−Ti.** PEO/H−Ti and PVP/H−Ti nanocomposites were prepared by adding

(9) Lemmon, J. P.; Wu, J.; Oriakhi, C. O.; Lerner, M. M. *Electrochim. Acta* **1995**, *13/14*, 2245.
(10) Carrado, K. A.; Xu, L. *Chem. Mater.* **1998**, *10*, 1440.
(11) Hild, A.; Séquaris J.-H.; Narres H.-D.; Schwuger, M. *Colloids Surf. A* **1997**, *123−124*, 515.
(12) Ogawa, M.; Inagaki, M.; Kodama, N.; Kuroda, K.; Kato, C. *J. Phys. Chem.* **1993**, *97*, 3819.
(13) Miyata, H.; Sugahara, Y.; Kuroda, K.; Kato, C. *J. Chem. Soc., Faraday Trans. 1* **1987**, *83*, 1851.
(14) Sukpirom, N.; Oriakhi, C. O.; Lerner, M. M. *Mater. Res. Bull.* **2000**, *3*, 325.
(15) Kerr, T. A.; Wu, H.; Nazar, L. F. *Chem. Mater.* **1996**, *8*, 2005.
(16) Wang, L.; Schindler, J.; Kannewurf, C. R.; Kanatzidis, M. G. *J. Mater. Chem.* **1997**, *7*, 1277.
(17) Nazar, L. F.; Wu, H.; Power, W. P. *J. Mater. Chem.* **1995**, *5*, 1985−93.
(18) Liu, Y.-J.; Schindler, J. L.; DeGroot, D. C.; Kannewurf, C. R.; Hirpo, W.; Kanatzidis, M. G. *Chem. Mater.* **1996**, *8*, 525.
(19) Oriakhi, C. O.; Nafshun, R. L.; Lerner, M. M. *Mater. Res. Bull.* **1996**, *12*, 1513.
(20) Gonzalez, G.; Santa Ana, M. A.; Benavente, E. *J. Phys. Chem. Solids* **1997**, *58*, 1457.
(21) Bissessur, R.; Kanatzidis, M. G.; Schindler, J. L.; Kannewurf, C. R. *J. Chem. Soc., Chem. Commun.* **1993**, 1582.
(22) Tsai, H.-L.; Schindler, J. L.; Kannewurf, C. R.; Kanatzidis, M. G. *Chem. Mater.* **1997**, *9*, 875.
(23) Yang, D.; Frindt, R. F. *J. Mater. Res.* **2000**, *11*, 2408.
(24) Oriakhi, C. O.; Lerner, M. *Chem. Mater.* **1996**, *8*, 2016.
(25) Jeevanandam, P.; Vasudevan, S. *Chem. Mater.* **1998**, *10*, 1276.
(26) Wang, L.; Rocci-Lane, M.; Brazis, P.; Kannewurf, C. R.; Kim, Y. I.; Lee, W.; Choy, J. H.; Kanatzidis, M. G. *J. Am. Chem. Soc.* **2000**, *28*, 6629.
(27) Matsuo, Y.; Tahara, K.; Sugie, Y. *Carbon* **1997**, *1*, 1113.
(28) Matsuo, Y.; Tahara, K.; Sugie, Y. *Carbon* **1996**, *5*, 672.
(29) Kojima, Y.; Usuki, A.; Kawasumi, M.; Okada, A.; Fukushima, Y.; Kurauchi, T.; Kamigaito, O. *J. Mater. Res.* **1993**, *8*, 1185.
(30) Fischer, H. R.; Gielgens, L. H.; Koster, T. P. M. *Acta Polym.* **1999**, *50*, 122.
(31) Manolis, L. *Plastics Technol.* **1999**, *45*, 52.
(32) Lan, T.; Kaviratna, P. D.; Pinnavaia, T. J. *Chem. Mater.* **1994**, *6*, 573.
(33) Gilman, J. W. *Appl. Clay Sci.* **1999**, *15*, 31.
(34) Serpone, N.; Lawless, D.; Khairutdinov, R.; Pelizzetti, E. *J. Phys. Chem.* **1995**, *99*, 16655.
(35) Kocher, M.; Daubler, T. K.; Harth, E.; Scherf, U.; Gugel, A.; Neher, D. *Appl. Phys. Lett.* **1998**, *72*, 650.
(36) Sasaki, T.; Watanabe, M. *J. Phys. Chem. B* **1997**, *101*, 10159.
(37) Yoshida, M.; Lal, M.; Kumar, N. D.; Prasad, P. N. *J. Mater. Sci.* **1997**, *32*, 4047.
(38) Zheng, M.-P.; Jin, Y.-P.; Jin, G.-L.; Gu, M.-Y. *J. Mater. Sci. Lett.* **2000**, *19*, 433.
(39) Hervieu, M.; Raveau, B. *Rev. Chim. Miner.* **1981**, *18*, 642.
(40) Sasaki, T.; Watanabe, M.; Michiue, Y.; Komatsu, Y.; Izumi, F.; Takenouchi, S. *Chem. Mater.* **1995**, *7*, 1001.
(41) Sasaki, T.; Nakano, S.; Yamauchi, S.; Watanabe, M. *Chem. Mater.* **1997**, *9*, 602.
(42) Sasaki, T.; Watanabe, M.; Hashizume, H.; Yamada, H.; Nakazawa, H. *J. Am. Chem. Soc.* **1996**, *118*, 8329.
(43) Sasaki, T.; Watanabe, M. *Mol. Cryst. Liq. Cryst.* **1998**, *311*, 417.
(44) Sasaki, T.; Watanabe, M. *J. Am. Chem. Soc.* **1998**, *120*, 4682.
(45) Sasaki, T.; Kooli, F.; Iida, M.; Michiue, Y.; Takenouchi, S.; Yajima, Y.; Izumi, F.; Chakoumakos, B. C.; Watanabe, M. *Chem. Mater.* **1998**, *10*, 4123.
(46) Sasaki, T.; Ebina, Y.; Watanabe, M.; Decher, G. *Chem. Commun.* **2000**, 2163.
(47) Grey, I. E.; Li, C.; Madsen, I. C.; Watts, J. A. *J. Solid State Chem.* **1987**, *66*, 7.

aqueous polymer solutions to stirred suspensions of the exfoliated H−Ti described above. In both cases, a 3 mol/mol ratio of polymer formula unit to protons in H−Ti was used to ensure that the polymer was present in excess. The solutions were acidified by adding aqueous HCl until gel formation was observed and then stirred for an additional 2 min. The gels were filtered, washed copiously with DI water, and dried under vacuum for 24 h. Alternately, the PVP/H−Ti gel was cast on a glass substrate and dried in air for 24 h to obtain a thin film.

**Characterization.** Powder X-ray diffraction (XRD) of all materials were obtained using a Siemens D5000 diffractometer and Cu Kα radiation (0.15418 nm) from 2° to 60° 2$\theta$ in 0.02° steps. Thermal analyses were performed at 10 °C/min under flowing $N_2$ (20 mL/min) using a Shimadzu TGA-50 and DSC-50. Infrared spectra were recorded on samples pressed into KBr disks using a Nicolet 510P FTIR spectrometer (resolution = 1 $cm^{-1}$, 64 scans averaged). Elemental (C/H/N/Ti) analyses were performed by Desert Analytics Laboratory (Tucson, AZ) and converted to the compositions $H_xTi_{2-x/4}O_4(TBA)_m(polymer)_n(H_2O)_p$ by setting $x = 0.7$ and assuming residual mass is due to oxygen. Microstructures were observed for samples coated with 60/40 Au/Pd using an Amray SEM operated at an accelerating voltage of 10.0 kV.

## Results and Discussion

As described previously, the layered titanate $H_x$-$Ti_{2-x/4}\square_{x/4}O_4 \cdot yH_2O$ ($x \approx 0.7$), H−Ti, is readily obtained by proton exchange from the Cs intercalate and slowly delaminates upon stirring with excess aqueous tetrabutylammonium (TBA).[44] The long processing time to obtain the stable colloidal suspension is inconvenient when using the exfoliated H−Ti as a precursor, but the suspension can be obtained from H−Ti within minutes by use of ultrasonic processing. These details will be reported separately.[48] In this work, a stable suspension of exfoliated H−Ti was obtained by ultrasonication of H−Ti in aqueous solution with TBA/H = 0.5 for 20 min.

When aqueous solutions of poly(ethylene oxide), PEO, or poly(vinylpyrrolidone), PVP, are added to a suspension of exfoliated H−Ti and the solution acidified to pH = 2, gels rapidly form and a solid precipitate can be obtained by filtration. These observations suggest the spontaneous aggregation of titanate sheets and polymer. Strong attractive Coulombic forces should arise between the negative titanate sheets and polymer in solution because PVP is positively charged at pH < 3.0−3.5[49] and PEO forms complexes with cations in aqueous solution.

Powder XRD patterns for the solid products obtained and the starting H−Ti phase are shown in Figure 1, and the derived basal repeat and stacking domain lengths are listed in Table 2. Because of preferred orientation of the platy particles, strong lines in these patterns are due to basal repeat reflections. H−Ti shows a basal repeat dimension of 0.93 nm, which indicates a monolayer of water intercalated along with protons between titania sheets.[40] After heating to 100 °C for 0.5 h, intercalate water is removed and the layer thickness for H−Ti can be obtained directly from the broadened peak at 0.68 nm in Figure 1b. This agrees well with the value obtained by considering the crystallographic data for the parent titanate:[47] the distance between surface O atoms (0.42 nm) plus the diameter of an oxide (0.28 nm) gives a single sheet thickness of about 0.70 nm. When the colloidal suspension is freeze-dried to obtain the solid product TBA/H−Ti, the stacking repeat dimension increases to 1.75 nm. This expansion of about 1.1 nm is consistent with intercalation of TBA between titanate sheets and matches the lamellar, turbostratic structure (repeat = 1.75 nm) previously obtained after long-term stirring and solid reaggregation in aqueous TBA solution.[44]

After reaction with the polymer-containing solutions, neither the starting H−Ti phase nor the TBA/H−Ti phase described above are observed in XRD of the solid precipitates. New stacking repeat lengths of 1.49 and 2.88 nm for PEO/H−Ti and PVP/H−Ti, respectively, indicate galleries with expanded dimensions relative to H−Ti. The intercalate layer dimension for PEO/H−Ti

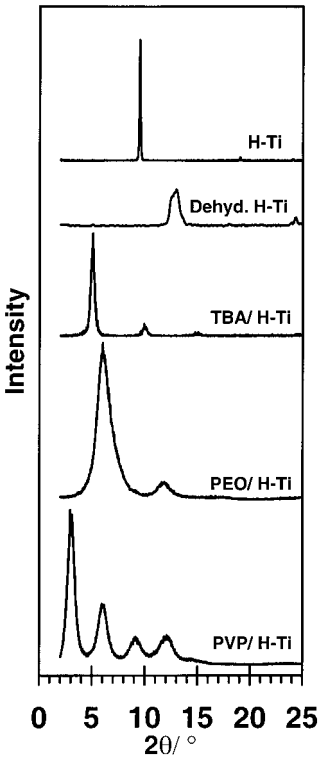


**Figure 1.** Powder X-ray diffraction patterns from samples. The inset for TBA/H−Ti is magnified *x* times and on a different degrees scale.

**Table 2. Basal Repeat and Stacking Domain Lengths for H−Ti, TBA/H−Ti, PEO/H−Ti, and PVP/H−Ti from Powder XRD Data**

| sample | basal repeat (nm) | stacking domain length[a] (nm) | sample | basal repeat (nm) | stacking domain length[a] (nm) |
|---|---|---|---|---|---|
| H−Ti | 0.93 | 80 | PEO/H−Ti | 1.49 | 6 |
| TBA/H−Ti | 1.75 | 20 | PVP/H−Ti | 2.88 | 8 |

[a] Determined using the Scherrer relation.[50]

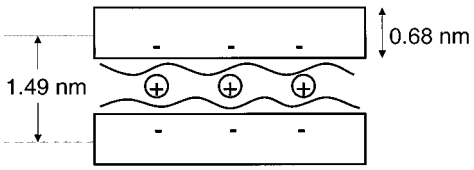


**Figure 2.** Structure scheme for PEO/H−Ti.

(48) Sukpirom, N.; Lerner, M., submitted for publication in *Mater. Sci. Eng. A.*

(49) Frank, H. P. *J. Polym. Sci.* **1954**, *12*, 565.

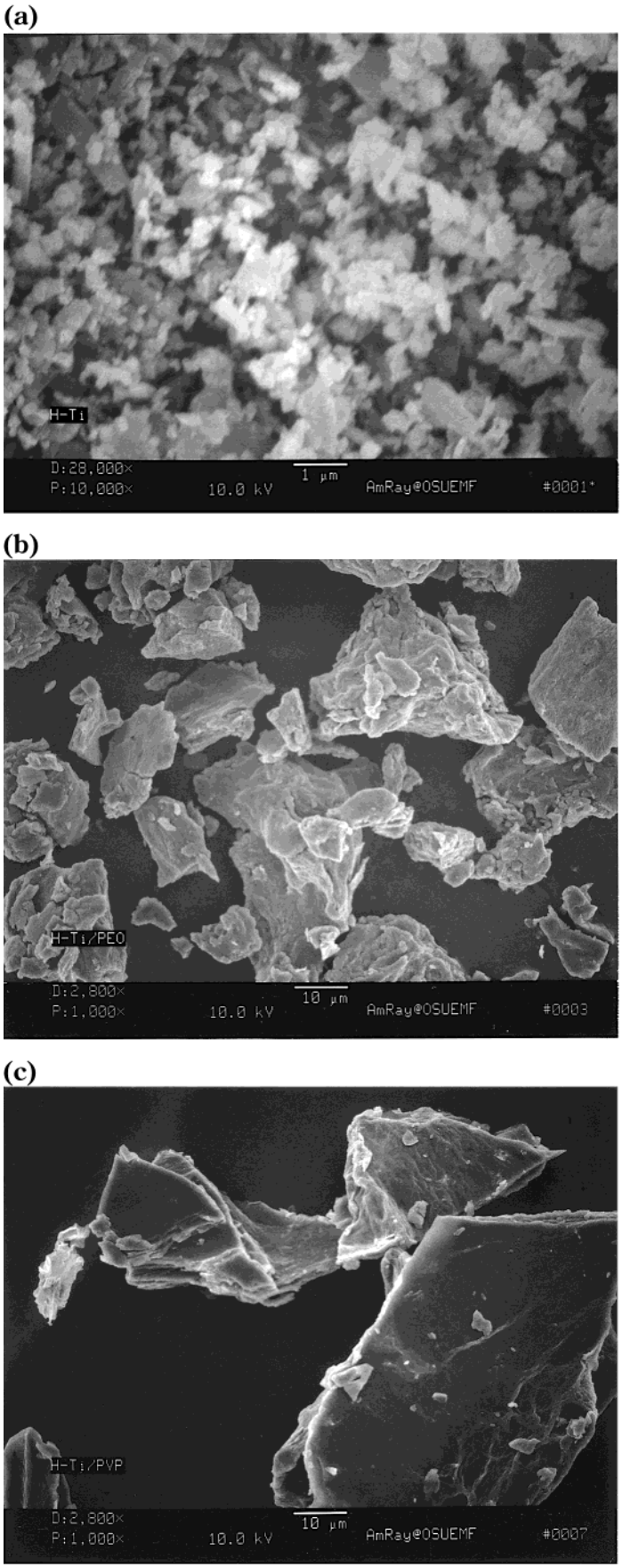


**Figure 3.** SEM images of (a) H−Ti, (b) PEO/H−Ti, and (c) PVP/H−Ti.

is 1.49−0.68 = 0.81 nm. For several layered hosts, the incorporation of a PEO bilayer has been shown to result in gallery dimensions of 0.8−0.9 nm.[9,18,24] A simple bilayer scheme for the PEO/H−Ti structure with PEO

**Table 3. FTIR Peak Positions and Assignments for H−Ti, PEO/H−Ti, PVP/H−Ti, and Starting Polymers (s = Strong, w = Weak, b = Broad, h = Shoulder)**

| H−Ti | PEO[a] | PEO/H−Ti | PVP[a] | PVP/H−Ti | TBA/H−Ti | assignment |
|---|---|---|---|---|---|---|
| 3423 bs | 3421 b | 3437 b | 3512 b | 3419 b | 3455 b | O−H str |
| 3217 bs | | | | | | |
| 1628 b | | 1653 w | | | 1654 bw | $OH_2$ bend |
| 921 h | | | | | 902 bw | Ti═O str |
| 676 h | | 693 h | | 684 b | 693 b | |
| 535 bs | | 447 bs | | 466 bs | 485 bs | Ti−O str |
| | 2950 h | 2942 b | 2955 b | 2965 | 2962 | C−H str |
| | | | 2939 h | | | C−H str |
| | 2888 s | 2873 | 2896 h | 2880 w | 2878 w | C−H str |
| | | | 1495 | 1494 w | 1488 w | $CH_2$ bend |
| | 1472 | 1457 | 1463 | 1463 | 1468 w | $CH_2$ bend |
| | | | 1423 s | 1424 | | $CH_2$ def |
| | 1342 | 1350 w | 1375 | 1365 | | $CH_2$ def |
| | 1296 | 1306 w | | | | C−C str |
| | 1227 | 1254 w | 1250 h | 1225 | | C−C str |
| | 1104 s | 1111 s | | | | C−O str |
| | | 1049 w | | | | |
| | 963 | | | | | C−C str |
| | 843 | | 849 | | | C−C str |
| | 529 bw | | | | | |
| | | | 1683 s | 1675 s | | C═O str |
| | | | 1289 s | 1289 | | C−N str |
| | | | 1168 w | | 1156 w | |
| | | | 739 w | | | |
| | | | 651 | | | |
| | | | 572 | | | |

[a] PEO assignments from ref 51; PVP assignments from refs 52 and 53.

bilayer is presented in Figure 2. PVP/H−Ti has a polymer gallery dimension of approximately 2.2 nm. With such a large dimension and limited structural information, the polymer arrangement cannot be deduced in this case Wang et al. reported an expansion of 3.2 nm for PVP incorporated between $MoO_3$ layers[16] and 2.3 nm for PVP galleries within $RuCl_3$ layers.[26] Carrado and Xu reported an expansion of 0.39−1.33 nm depending on the amount of PVP incorporated into PVP/hectorite nanocomposites.[10] Other studies[12,13] showed expansions of 1.34 and 1.38 nm for PVP incorporated into mica and montmorillonite.

SEM images of particle microstructures for H−Ti, PEO/H−Ti, and PVP/H−Ti are shown in Figure 3. The H−Ti has a platy morphology with platelet diameters of 0.1−1 $\mu$m. PEO/H−Ti and PVP/H−Ti consist of much larger aggregates, with particle diameters in the range of 10−100 $\mu$m. The formation of a gel and subsequent drying process appears to generate these larger particles.

The presence of PEO and PVP in the nanocomposites was confirmed by FTIR. Spectra from H−Ti, TBA/H−Ti, PEO/H−Ti, PVP/H−Ti, and the starting polymers are shown in Figure 4, and a summary of peak positions and assignments is provided in Table 3. H−Ti has a broad peak with a maximum at 3425 $cm^{-1}$, with a shoulder at 3220 $cm^{-1}$. The broad peak can be ascribed to an O−H stretching vibration either for $H_2O$ (or $H_3O^+$) that is strongly associated with the layer surface; the peak position for $H_2O$ without strong hydrogen bonding

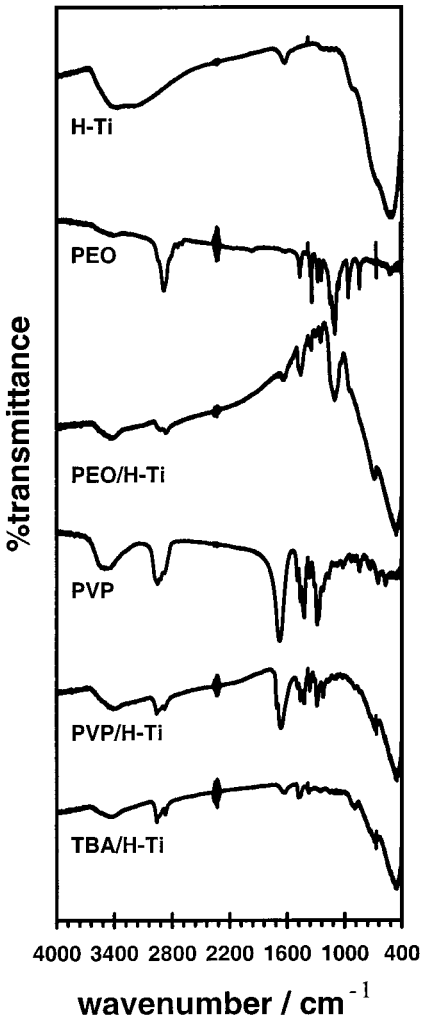


**Figure 4.** FTIR spectra for powder samples in KBr pellets. Peak positions are summarized in Table 3.

(50) Cullity, B. D. *Elements of X-ray Diffraction, 2nd Ed.*; Addison-Wesley: Reading, MA, 1978.
(51) Yoshihara, T.; Tadokoro, H.; Murahashi, S. *J. Chem. Phys.* **1964**, *41*, 2902.
(52) *The Infrared Spectra Atlas of Monomers and Polymers*; Sadler Research Laboratories: Philadelphia, PA, 1980.
(53) Cohen Stuart, M. A.; Fleer, G. J.; Bijsterbosch, B. H. *J. Colloid Interface Sci.* **1982**, *90(2)*, 321.

**Table 4. Thermal Analysis Data for H−Ti, PEO/H−Ti, PVP/H−Ti, and TBA/H−Ti**

| | temp (°C) | mass loss (%) | DSC peak |
|---|---|---|---|
| **H−Ti** | 40−120 | 10.8 | endo, vs |
| | 160−400 | 3.9 | exo, m (160−300 °C) |
| | | | exo, m (350−400 °C) |
| | 400−600 | 1.5 | exo, s |
| **PEO/H−Ti** | 30−150 | 4.4 | endo, m |
| | 220−320 | 15.7 | exo, vs (220−400 °C) |
| | 400−470 | 4.7 | exo, m |
| | 500−570 | 2.2 | exo |
| **PVP/H−Ti** | 30−160 | 7.4 | endo, s |
| | 175−240 | 3.5 | endo, w |
| | 270−400 | 7.1 | exo, s |
| | 400−485 | 15.8 | exo, vs |
| | 540−610 | 19.4 | exo |
| **TBA/H−Ti** | 30−130 | 6.0 | endo, s |
| | 130−180 | 12.1 | endo, m |
| | 185−230 | 4.8 | endo, w |
| | 230−320 | 9.6 | exo, vs (230−405 °C) |
| | 330−440 | 2.5 | exo, w (405−440 °C) |
| | 440−560 | 4.5 | exo |

should lie above 3600 $cm^{-1}$.[54] The shoulder at 3220 $cm^{-1}$ can be ascribed to an overtone of the $H_2O$ bending mode at about 1630 $cm^{-1}$. In TBA/H−Ti, PEO/H−Ti, and PVP/H−Ti, the broad O−H peak appears at reduced intensity, indicating a decreased water content in the solid. The O−H peak positions for these three samples (at 3455, 3437, and 3512 $cm^{-1}$, respectively) indicate strong water association with the layer surfaces.

H−Ti has a strong, broad vibration at 535 $cm^{-1}$, which shifts to lower wavenumbers in TBA/H−Ti, PEO/H−Ti, and PVP/H−Ti. This absorption peak can be ascribed to the Ti−O (bridging) vibration, which gives rise to a strong broad peak centered around 600 $cm^{-1}$ in anatase $TiO_2$. The shifted position for this vibration may be related to a decrease in hydrogen bonding at the titanate surface as a result of the gallery expansion after intercalation of TBA, PEO, or PVP. The Ti═O (apical) stretching mode is tentatively assigned to the shoulder observed near 920 $cm^{-1}$. For comparison, this mode occurs near 1000 $cm^{-1}$ in layered vanadates.[55] The mode is not clearly seen in the nanocomposites prepared.

The FTIR spectrum for PEO/H−Ti exhibits the $CH_2$ stretching, bending, and other deformation modes present in PEO at 2942, 2987, 1457, and 1350 $cm^{-1}$. The shifted peak positions relative to those for the neat polymer could suggest a more anisotropic conformation for the PEO intercalate,[26,56] although the greater peak widths and lower peak intensities in the nanocomposites probably do not support any detailed analysis in this case. Strong absorption due to the C−O stretching vibration is observed at 1111 $cm^{-1}$ in PEO/H−Ti. PVP/H−Ti shows absorbances from alkyl groups as well as prominent carbonyl and C−N stretching vibrations at 1675 and 1289 $cm^{-1}$. These peaks are at similar positions to those for PVP itself.

Figure 5 and Table 4 present the TGA and DSC traces and data for the solid products obtained. In agreement

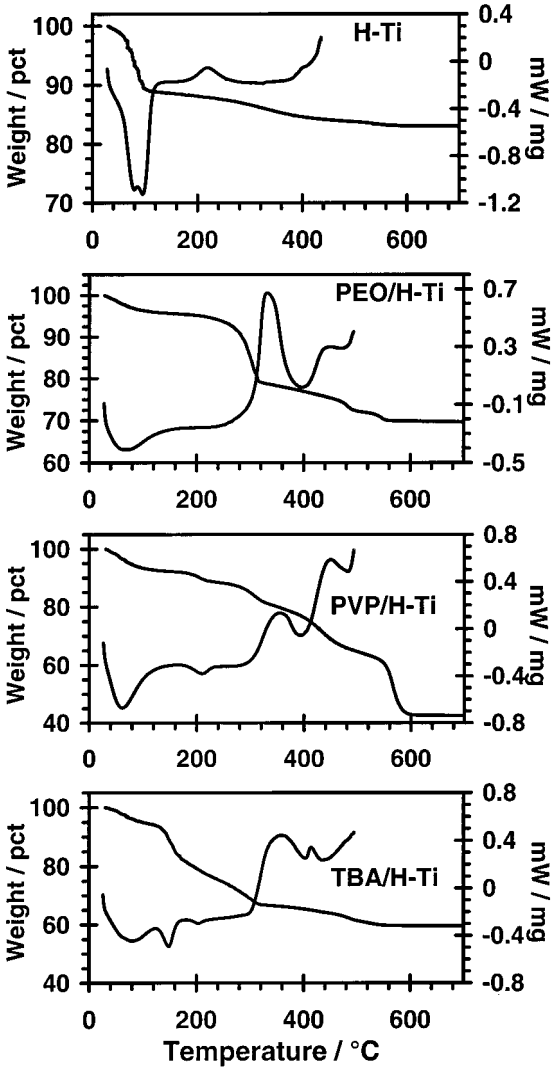


**Figure 5.** TGA and DSC traces obtained at 10 °C/min under flowing $N_2$.

with previous results,[40] H−Ti loses approximately 10 wt % from ambient temperature to 120 °C and a further 5 wt % after heating to high temperature. The losses correspond to endothermic and slightly exothermic events, respectively, and have been ascribed to loss of intercalate water (with retention of a protonated layer structure), followed by water loss (with sheet degradation) to form a disordered product. The disordered structure rearranges to form anatase above 450 °C. The thermal degradation is summarized by the following reaction steps:

$$H_xTi_{2-x/4}\square_{x/4}O_4{\cdot}yH_2O \rightarrow H_xTi_{2-x/4}\square_{x/4}O_4 + yH_2O \quad (1a)$$

$$H_xTi_{2-x/4}\square_{x/4}O_4 \rightarrow (2-x/4)TiO_2(\text{amorphous}) + (x/2)H_2O \quad (1b)$$

$$TiO_2(\text{amorphous}) \rightarrow TiO_2(\text{anatase}) \quad (1c)$$

The mass losses provide an approximate composition of $H_{0.6}Ti_{1.85}O_4{\cdot}1.03H_2O$, which indicates a intercalate water monolayer, and a proton content similar to that expected.

PEO/H−Ti shows an endothermic loss of approximately 4 wt % below 120 °C, again ascribed to interca-

(54) *The Infrared Spectra of Minerals*; Farmer, V. C., Ed.; Mineralogical Society: London, 1974.
(55) Huguenin, F.; Gambardella, M.; Torresi, R.; Torresi, S.; Butty, D. *J. Electrochem. Soc.* **2000**, *147*, 2437.
(56) Montarges, E.; Michot, L. J.; Lhote, F.; Frabien, T.; Villieras, F. *Clays Clay Miner.* **1995**, *43*, 417.

**Table 5. Compositional Analyses for H−Ti, PEO/H−Ti, PVP/H−Ti, and TBA/H−Ti**

| | | weight percent | | | | | | | |
|---|---|---|---|---|---|---|---|---|---|
| sample | | C | H | N | Ti | TBA | polymer | $H_2O$ | empirical formula |
| **PEO/H−Ti** | obs | 15.32 | 3.09 | 0.71 | 35.88 | | | | |
| | calc | 15.86 | 4.01 | 0.06 | 35.60 | 1.0 | 27.6 | 9.4 | $H_{0.7}Ti_{1.83}O_4(C_{16}H_{36}N)_{0.01}(C_2H_4O)_{1.54}(H_2O)_{1.28}$ |
| **PVP/H−Ti** | obs | 30.82 | 4.80 | 5.59 | 27.67 | | | | |
| | calc | 30.77 | 4.86 | 5.63 | 27.65 | 3.6 | 43.0 | 5.2 | $H_{0.7}Ti_{1.83}O_4(C_{16}H_{36}N)_{0.05}(C_6H_9NO)_{1.22}(H_2O)_{0.92}$ |
| **TBA/H−Ti**[a] | obs | 24.5 | 5.1 | 1.6 | 36.5 | | | | |
| | calc | 24.3 | 5.5 | 1.8 | 36.8 | 30.6 | | 5.3 | $H_{0.7}Ti_{1.83}O_4(C_{16}H_{36}N)_{0.3}(H_2O)_{0.7}$ |

[a] Data from ref 41.

late water loss. A strong exotherm and mass loss from 220 to 320 °C is ascribed predominantly to polymer decomposition, although the titania sheets may also degrade in this temperature range. The sum of polymer and water contents determined by elemental analyses is 38 wt % (see below), which is somewhat larger than that obtained by gravimetry to 900 °C (31 wt %).

The TGA trace for H−Ti/PVP is similar to that reported for the $TiO_2$/PVP nanocomposite prepared by Zheng et al.[38] Losses below 250 °C can be ascribed to intercalate water loss. Above 250 °C, a complex series of exothermic degradation steps ensues. For comparison, decomposition of pure PVP begins at about 340 °C. The total weight loss to 900 °C (58 wt %) is consistent with the sum of TBA, polymer, and water contents determined by elemental analyses (54 wt %).

Elemental (C/H/N/Ti) analyses are indicated in Table 5 and give compositions of $H_{0.7}Ti_{1.83}O_4(C_2H_4O)_{1.54}(H_2O)_{1.28}$ for PEO/H−Ti and $H_{0.7}Ti_{1.83}O_4(C_{16}H_{36}N)_{0.05}(C_6H_9NO)_{1.22}(H_2O)_{0.92}$ for PVP/H−Ti. The TBA contents in the polymer-containing samples were very low compared with that for TBA/H−Ti, which contains 31 wt % TBA. The XRD data indicate that no TBA/H−Ti phase is present, and these analytical results further indicate that little TBA is present in the polymer-occupied galleries. The intercalated water content indicates that the water/proton mole ratio increases only a small amount relative to that in H−Ti, so that most of the intercalated water could be associated with intercalate protons to make hydronium cations, as is the case in H−Ti.

## Conclusion

PEO and PVP/titanate-layered nancomposites can be prepared by (1) exfoliating layered titanates in aqueous TBA solutions and (2) acidifying to form a gel. Structural characterization indicates that the PEO nanocomposites have polymer bilayers within titanate galleries. FTIR and thermal analyses indicate a reduced TBA and water content relative to the intercalation compounds formed without polymer.

**Acknowledgment.** The authors gratefully acknowledge support from NSF Grant DMR-9900390 and helpful advice from Dr. Takayoshi Sasaki at NIRIM and Dr. Christopher Oriakhi at Hewlett-Packard. N.S. acknowledges support from the Royal Thai Government.

CM0101226